

# Theory of magnetic domains in uniaxial thin films

**F. Viot<sup>1</sup>, L. Favre<sup>1</sup>, R. Hayn<sup>1</sup> and M. D. Kuz'min<sup>2</sup>**

<sup>1</sup>IM2NP, Aix-Marseille Univ., Faculté St. Jérôme, Case 142, F-13397 Marseille Cedex 20, France

<sup>2</sup>IFW Dresden, P.O. Box 270 116, D-01171 Dresden, Germany

## **Abstract.**

For uniaxial easy axis films, properties of magnetic domains are usually described within the Kittel model, which assumes that domain walls are much thinner than the domains. In this work we present a simple model that includes a proper description of the magnetostatic energy of domains and domain walls and also takes into account the interaction between both surfaces of the film. Our model describes the behavior of domain and wall widths as a function of film thickness, and is especially well suited for the strong stripe phase. We prove the existence of a critical value of magneto-crystalline anisotropy above which stripe domains exist for any film thickness and justify our model by comparison with exact results. The model is in good agreement with experimental data for *hcp* cobalt.

PACS numbers: 75.60.Ch, 75.70.Kw, 75.30.Gw

Submitted to: *J. Phys. D: Appl. Phys.*

## 1. Introduction

Thin magnetic films with stripe domains and perpendicular magneto-crystalline anisotropy present a high scientific interest. They are model systems to understand the domain structure of ferromagnetic, as well as ferroelectric, thin films. Such materials are used for the fabrication of memories and spin injection devices. Considering a thin film with its bulk easy axis perpendicular to the surface, the magnetization direction in the domains can depend on the film thickness. Thick films behave as bulk material but for thin films, the competition between exchange, magnetostatic and magneto-crystalline energy can tip up the magnetization into the plane. A very well known theory of magnetic domain structure has been developed by Kittel [1]. In this model, the film magnetization is described by a square profile. Domain wall energy is allowed for the energy balance, but not for the magnetization profile, which determines the magnetostatic energy. Such an approximation is only valid when the domain width is much larger than the width of domain walls. Therefore, this model is bound to fail for very thin films, where the domain width vanishes. Furthermore, the magnetostatic interaction between the top and bottom surfaces is disregarded, which leads to wrong results unless the domain width is much less than the film thickness. The latter does not hold for very thin strongly anisotropic films.

Within the Kittel model, the width of stripe domains is proportional to the square root of the film thickness. The model also predicts the existence of a critical film thickness below which the magnetization direction flips from out-of-plane to in-plane direction. Later on, it was shown that for materials with strong magneto-crystalline anisotropy  $K$  (in comparison to the square of the saturation magnetization  $M_0$ ) the magnetostatic interaction energy between top and bottom interface cannot be neglected. The ratio  $2K/(\mu_0 M_0^2)$  (in SI units) is also known as the quality factor  $Q$  and the magnetization direction remains perpendicular to the surface for all values of film thickness for  $Q > 1$ . Numerous theoretical and experimental works have been devoted to such materials with strong perpendicular magnetic anisotropy [2, 3, 4]. It has been shown that in such materials the domain width has a minimum as a function of film thickness, increasing towards smaller or larger thicknesses. Materials with strong perpendicular anisotropy are also of technological importance in the field of magnetic multilayers (see [5] and references therein).

Just above the critical film thickness, the magnetization still lies predominantly in the plane of the film, deviations from the homogeneous in-plane orientation being very small. This permits an exact mathematical solution of the problem of stripe domain nucleation at the critical point [6]. Near the critical point the out-of-plane component of the magnetization remains much smaller than the saturation value  $M_0$  and there is a strong variation of the magnetization direction across the film thickness. The corresponding phase is usually called the weak stripe phase. As the film thickness increases, the magnetization direction in the domains tends more and more towards the bulk easy axis, which is perpendicular to the film. Gradually, the weak stripe phase evolves towards the strong stripe phase, where the magnetization magnetization is predominantly parallel (or antiparallel) to the bulk easy axis.

For a detailed analysis of the weak stripe phase a micromagnetic numerical analysis is indispensable (see [7, 8, 9, 10] and many other works). However, simple analytical models are helpful for getting a quick, albeit crude understanding of the stripe phases. These models restrict the magnetization direction to the vertical plane parallel to the stripes (i.e. they consider domain walls of Bloch type) but

improve the Kittel model. One can distinguish between models with a linear domain wall profile [11] or others which use the Jacobi sine function to parametrize the magnetization profile [12, 13]. Also a sinewave magnetization profile was proposed by Saito [14] to treat the weak stripe phase in an approximate manner. In the following we present a thorough analytical and numerical analysis of a simple but quite complete model for the strong stripe phase. We adopt a sinewave magnetization profile in the wall and we take into account the magnetostatic interaction between the top and bottom surfaces of the film. Our model applies to hexagonal Co, for which a critical thickness between 25 nm [15, 16] and 40 nm [17] has been reported, as well as to materials with high magneto-crystalline anisotropy, such as FePd(001) or garnet films [4, 17, 18]. Another possible application concerns ferromagnetic thin films of  $\text{Mn}_5\text{Ge}_3$  that were recently synthesized [19, 20]. Our model unifies previous results for materials with strong anisotropy ( $Q > 1$ ) [2, 3, 4] and those with medium anisotropy ( $\frac{1}{2} \lesssim Q < 1$ ) [11], containing them as special cases. The explicit treatment of the domain wall is an important improvement with respect to the Kittel model since it allows the determination of the in-plane remanent magnetization, which is important for the analysis of experimental data. We give numerical results for the dependence of domain and wall widths on the film thickness and calculate the critical thickness at which the magnetization switches from out-of-plane to in-plane direction if  $Q < 1$ . We show that the critical thickness tends to zero as  $Q \rightarrow 1$ . This behavior is identical in our model and in the exact solution [6]. In the case of strong anisotropy ( $Q > 1$ ) stripe magnetic domains exist at any film thickness.

Our theory considers a non-magnetostrictive film: the magneto-elastic energy is equal to zero. Moreover, the surface anisotropy is neglected. It is not suited for materials where the surface anisotropy plays an important role. We concentrate on the strong stripe phase since the details of the weak stripe phase are hard to capture in a simple model. In materials with high anisotropy the weak stripe phase does not appear at all and it will be shown below that even in materials with medium anisotropy ( $\frac{1}{2} \lesssim Q < 1$ ) it is of rather limited importance. In the latter case the weak stripe phase occurs only in a narrow interval of thicknesses around the critical point. This region of the weak stripe phase is not correctly described in our model. On the other hand, even in the case of weak anisotropy ( $Q \ll 1$ ), our model provides a correct qualitative description of the strong stripe phase, although it neglects such important phenomena as closure domains.

Our paper is organized as follows. After a short summary of known results (Kittel's theory, sawtooth magnetization model, exact results for stripe phase nucleation) we present our model in Section 3. In Section 4 we show its analytical and numerical solution. The usefulness of our theory is demonstrated in Section 5 by way of theoretical analysis of published experimental data for the well-known *hcp* cobalt system. In Section 6 we compare our model with other approaches and expose its strengths and limitations.

## 2. Known results

### 2.1. Kittel's model

This model was developed for ferromagnetic films with uniaxial anisotropy perpendicular to the film. It determines the width of magnetic stripe domains  $d$  as a function of the film thickness  $h$ , and the critical thickness where the magnetization

direction flips from out-of-plane to in-plane (see Fig. 1). The total energy density (per

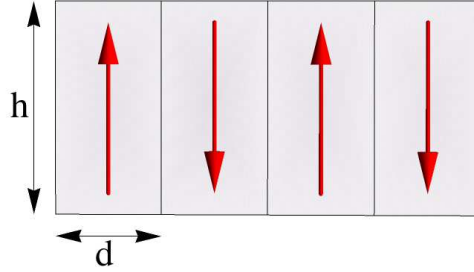


Figure 1: Kittel model for ferromagnetic thin films with uniaxial anisotropy.

unit volume) is given by:

$$E_{\text{total}} = 0.136\mu_0 M_0^2 \frac{d}{h} + \frac{\sigma}{d}, \quad (1)$$

where  $M_0$  denotes the saturation magnetization and  $\sigma$  the surface wall energy. The latter is obtained in a separate variational calculation for an isolated Bloch wall [21],  $\sigma = 4\sqrt{AK}$ , where  $A$  is the exchange stiffness constant. The same calculation yields the wall width,  $\delta = \pi\sqrt{A/K}$ . It is convenient to express all spatial dimensions in the units of  $\sqrt{A/K}$ :

$$\tilde{h} = \frac{h}{\sqrt{A/K}}, \quad \tilde{d} = \frac{d}{\sqrt{A/K}}, \quad \tilde{\delta} = \frac{\delta}{\sqrt{A/K}}. \quad (2)$$

Thus, Kittel's reduced wall width is a constant,

$$\tilde{\delta} = \pi. \quad (3)$$

The only essential material parameter in the model is the dimensionless quality ratio,  $Q = 2K/(\mu_0 M_0^2)$ . The first term of Eq. (1) refers to the magnetostatic energy of a rectangular domain profile, neglecting the influences of finite wall width and film thickness. Therefore, strictly speaking, the Kittel model is only applicable when the following strong inequalities hold:

$$\delta \ll d \ll h, \quad (4)$$

or alternatively,  $\tilde{\delta} \ll \tilde{d} \ll \tilde{h}$ . The right-hand condition ensures the negligibility of the magnetostatic interaction between the top and the bottom surfaces of the film. By minimizing the energy, one obtains the equilibrium domain width:

$$\tilde{d} = 3.84\sqrt{Q\tilde{h}}, \quad (5)$$

and the minimum energy density:

$$E_{\text{total}}^{\min} = 2\sqrt{\frac{0.136\mu_0 M_0^2 \sigma}{h}}. \quad (6)$$

As one can see, the minimum energy density  $E_{\text{total}}^{\min}$  tends to infinity as  $h \rightarrow 0$ . Therefore, the multi-domain structure cannot be stable in that limit within the Kittel model. Indeed, for a uniform in-plane magnetization (perpendicular to the bulk easy axis), the magnetostatic and the exchange energies are equal to zero, and the

anisotropy energy is maximal and equal to  $K$ . The critical point is obtained by equating Eq. (6) to  $K$ . Therefore, we can express the reduced critical thickness as follows:

$$\tilde{h}_c'' = 4.35Q^{-1}. \quad (7)$$

Within the Kittel model, the domain width is identical to the half-period  $d$  (see Fig.1). Its value at the critical point is obtained by setting Eq. (7) into (5), which results in:

$$\tilde{d}_c'' = 8. \quad (8)$$

These equations permit to obtain a qualitative evaluation of the critical quantities. But they fail in the neighborhood of the critical thickness, where domain and wall widths become close, cf. Eqs. (3) and (8). Furthermore, by Eqs. (7) and (8) in the critical region the ratio  $h/d$  equals  $0.544/Q = 0.272\mu_0 M_0^2/K$ , i.e. also the second precondition of the Kittel model (4) is violated in the case of large anisotropy or small magnetization,  $Q \gtrsim 1$ . As a result, Kittel's model makes a wrong prediction for large  $Q$ : according to Eq. (7),  $\tilde{h}_c''$  decreases asymptotically, remaining nonzero at any finite  $Q$ . In actual fact, the critical thickness should vanish at  $Q = 1$ , as shown by rigorous calculations [6].

For that reason we decided to develop a model that would not break down in the strong-anisotropy case, by allowing for the electrostatic interaction between the top and bottom surfaces of the film and taking into account the wall width explicitly. Within that improved model we have obtained a good description of domain and wall width variation as a function of the film thickness (see Section 3).

## 2.2. Sawtooth magnetization model

The main goal of Kittel's model is the description of the strong stripe phase. Yet there is no direct transition between strong stripes and planar magnetization. Rather, it proceeds via an intermediate weak stripe configuration. The latter can be described by sawtooth magnetization model [14]. In this model the canting angle of the magnetization out of the homogeneous in-plane direction,  $\Theta(x)$ , is assumed to be a saw-tooth curve with a maximum value of  $\Theta_0$  and a minimum value of  $-\Theta_0$ ,  $\Theta_0 < \pi/2$ . Between the extrema the variation is linear and the half period is denoted by  $d$ . The sawtooth magnetization model is an approximate one, since it neglects the variation of the magnetization direction across the film thickness. The magnetostatic interaction between the top and bottom surfaces is not taken into account either. From the equation for the total energy below one can obtain the expression for the critical thickness where the magnetization starts to flip out-of-plane by a small deflection angle. The first part of the total energy corresponds to the magnetostatic energy;  $C_0$  is the leading coefficient of the Fourier series obtained from periodic profile of the deflection angle. The maximum angle  $\Theta_0$  is a variational parameter,  $0 < \Theta_0 < \pi/2$ .

$$E_{\text{total}} = \frac{\mu_0 M_0^2 C_0^2 d}{4\pi h} + \frac{4\Theta_0^2 h}{d} + \frac{K}{2} \left( 1 + \frac{\sin 2\Theta_0}{2\Theta_0} \right) \quad (9)$$

with  $C_0 = \frac{2\Theta_0 \cos \Theta_0}{\pi^2/4 - \Theta_0^2}$ .

The critical thickness is expressed as :

$$\tilde{h}_c''' = 27(2/\pi)^5 Q^{-1} = 2.82Q^{-1}. \quad (10)$$

The expression above has the same form as Kittel's critical thickness  $\tilde{h}_c''$ , Eq. (7), but with a smaller pre-factor. This opens up a possibility to interpret  $\tilde{h}_c''$  and  $\tilde{h}_c'''$  as the upper and lower bounds of an interval where the weak stripe phase exists. The latter is a transitional state between the homogeneously magnetized in-plane configuration, stable below  $\tilde{h}_c'''$ , and Kittel's *strong* stripe domain structure, taking place above  $\tilde{h}_c''$ . One observes the 'wrong' behavior of  $\tilde{h}_c'''(Q)$  at  $Q > 1$ , similar to that of  $\tilde{h}_c''(Q)$ . Eq. (10) also misbehaves at  $Q \ll 1$ . Rigorous calculations show (see Section 2.3) that the true lower bound of the weak stripe phase does not diverge as  $Q \rightarrow 0$ .

### 2.3. Exact description of stripe domain nucleation

The exact solution of the nucleation problem was given in 1961 by Muller [6]. A modern presentation, summarized here, can be found in the book of Hubert and Schäfer [7]. The theory was formulated for a thin magnetic film (thickness  $h$ , magnetization  $M_0$ ) with uniaxial anisotropy perpendicular to the film (anisotropy constant  $K$ ). The energy expression contains the magnetostatic energy, the exchange (stiffness  $A$ ) and anisotropy contributions; the theory imposes no restrictions on the magnetization direction. Below the critical thickness  $h_c$  the magnetostatic energy forces the magnetization into the plane of the film. At  $h = h_c$  there is an instability and the weak stripe phase emerges. In the neighbourhood of the critical point, deviations from a homogeneous in-plane orientation of magnetization are small, which allows to linearize the system of micromagnetic equations and find the exact analytical form of the instability mode. The reduced critical thickness  $\tilde{h}_c$  is a universal function of the quality ratio  $Q$ , see Fig. 4 (solid line). (The quantity plotted in the original drawing, Fig. 3.109a of Ref. [7], is a factor  $2\pi$  smaller.) At the same time, the critical half-period  $d_c$  can be found, as well as the distribution of magnetization directions in the critical mode. In the weak-anisotropy limit,  $Q \rightarrow 0$ , both  $\tilde{h}_c$  and  $\tilde{d}_c$  tend to the same finite value,

$$\tilde{h}_c \rightarrow \tilde{d}_c \rightarrow 2\pi. \quad (11)$$

As  $Q$  increases, the critical thickness  $h_c$  decreases and vanishes at  $Q = 1$ , whereas  $d_c$  diverges at that point. The exact results will be used later on to judge the validity of the sinewave wall model.

### 3. Sinewave wall model (SWM)

We propose a model stripe domain structure as shown in Figs. 2 and 3. Like in Kittel's model, the half-period is denoted by  $d$ , but it now includes a domain wall of width  $\delta$  (see Fig. 2). The inner domains, with constant magnetization equal to  $\pm M_0$ , have a width of  $d - \delta$ . The walls separating different domains are assumed to be of Bloch type, with linear variation of the angle  $\Theta(x)$  between the magnetization direction and the  $y$ -axis. This results in a magnetization profile of sinewave form, which is a good approximation of the profile obtained by the variational method. The schematic representation in Fig. 2 shows that we consider parallel stripe domains infinite in the  $y$  direction. In the  $x$  direction, the periodic magnetization profile is as shown in Fig. 3. The  $z$  dimension is restricted to the film thickness  $h$ .

To calculate the magnetostatic energy, we use an analogy with the electrostatic field calculation for alternating, positively and negatively, charged stripes (see Landau-Lifschitz [22]). We consider the realistic magnetization profile of Fig. 3 (as opposed

to a simple rectangular meander) as well as the magnetostatic interaction between the top and bottom surfaces of the film.

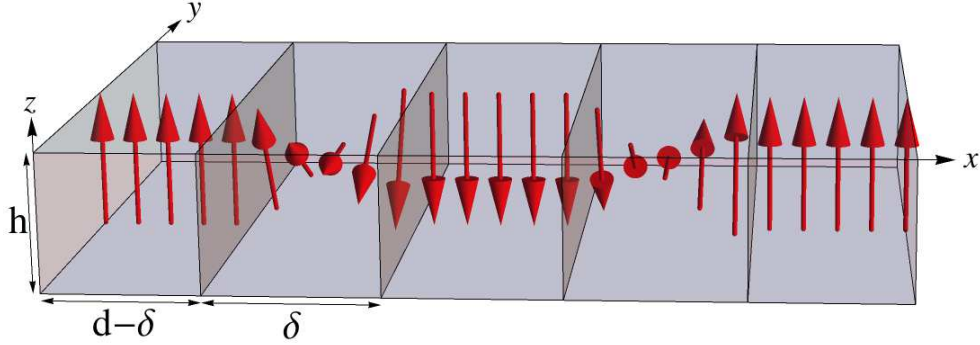


Figure 2: Sketch of periodic stripe domains in a magnetic thin film with domain walls of finite thickness.

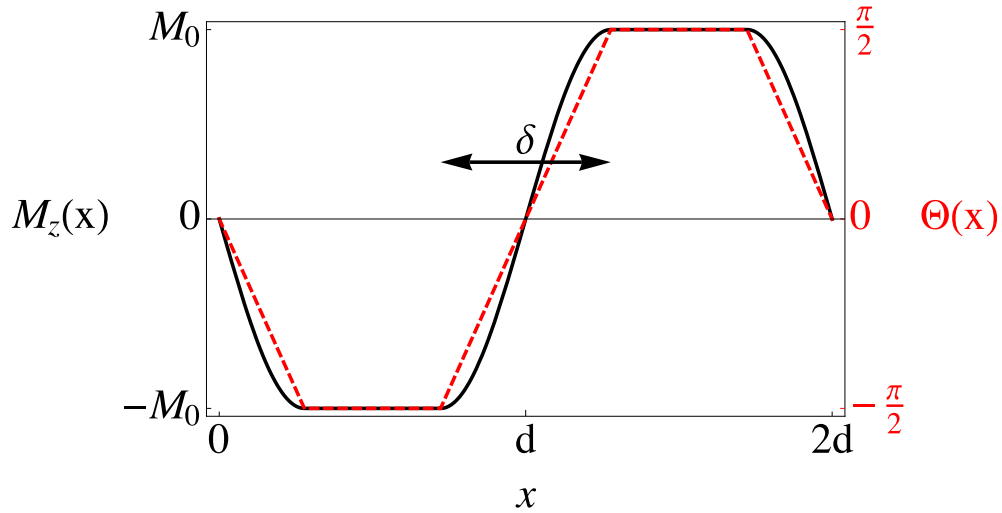


Figure 3: (color online) One full period of the domain structure of Fig. 2.  $M_z(x)$  (solid line) denotes the  $z$  component of the film magnetization, and  $\Theta(x)$  is the angle between the magnetization direction and the film surface (dashed line). The domain wall width is denoted by  $\delta$ .

The magnetostatic energy density (per volume) can be written as:

$$E_{\text{mag}} = \frac{\mu_0 d}{\pi h} \sum_{k=1}^{\infty} \frac{|C_k|^2}{k} \left[ 1 - \exp\left(-\pi k \frac{h}{d}\right) \right] \quad (12)$$

$$\text{with } C_k = \frac{2M_0}{k\pi [1 - k^2(\delta/d)^2]} \cos\left(\frac{k\pi\delta}{2d}\right) \quad (13)$$

where  $k$  is an odd number,  $C_k$  is the Fourier coefficient of  $M_z(x)$  (see Fig. 3). The domain structure is determined by the interplay between magnetostatic, exchange and anisotropy energies. The latter two contributions are as follows:

$$\begin{aligned} E_{\text{exch}} &= \frac{1}{2d} \int_0^{2d} A \left( \frac{d\Theta}{dx} \right)^2 dx \\ &= \frac{\pi^2}{d\delta} A \end{aligned} \quad (14)$$

$$\begin{aligned} E_{\text{aniso}} &= \frac{1}{2d} \int_0^{2d} K \cos^2[\Theta] dx \\ &= \frac{\delta}{2d} K \end{aligned} \quad (15)$$

The half-period  $d$  and the wall width  $\delta$  are then calculated by minimizing the total energy,

$$E_{\text{total}} = E_{\text{mag}} + E_{\text{exch}} + E_{\text{aniso}}. \quad (16)$$

Since it is not possible to solve analytically the two variational equations  $\partial_d E_{\text{total}} = 0$ ,  $\partial_\delta E_{\text{total}} = 0$  in the general case, we use a Nelder-Mead numerical method. The results are presented in the next Section.

## 4. Analytical and numerical results

### 4.1. Large film thickness

Before presenting the numerical solution in the general case let us discuss some specific situations. For sufficiently thick films the strong inequalities (4) are fulfilled and the expression for the Fourier coefficients, Eq. (13), becomes:

$$C_k = \frac{2M_0}{k\pi}. \quad (17)$$

Then Kittel's form is recovered for the magnetostatic energy density:

$$E_{\text{mag}} = \frac{4\mu_0 M_0^2 d}{\pi^3 h} \sum_{k=1}^{\infty} k^{-3} = 0.136\mu_0 M_0^2 \frac{d}{h}. \quad (18)$$

The wall energy associated with the above magnetostatic expression is a minimum for the following reduced wall width:

$$\tilde{\delta}_\infty = \pi\sqrt{2}. \quad (19)$$

The corresponding surface wall energy,  $\sigma = \pi\sqrt{2}\sqrt{AK}$ , is slightly (11%) larger than the variational result,  $4\sqrt{AK}$ , because of the imposed sinewave wall profile of  $M_z(x)$ . In the thick-film limit the dependence of the domain width on film thickness can be expressed analytically,

$$\tilde{d} = 4.05\sqrt{Q\tilde{h}}, \quad (20)$$

and is very similar to the result of the Kittel model, Eq. (5).



#### 4.2. Critical thickness and critical anisotropy

As the film thickness is reduced, the domain width  $d$  decreases and the wall width  $\delta$  increases. Just above the critical thickness, the magnetization profile is purely sinewave ( $\delta \rightarrow d$ ), forming an unstable spiral magnetic configuration. In this limit Eq. (12) can be simplified: the sum disappears since only the leading term of the Fourier series, with  $k = 1$ , survives. The magnetostatic energy becomes:

$$E_{\text{mag}} = \frac{\mu_0 M_0^2 d}{4\pi h} \left[ 1 - \exp\left(-\pi \frac{h}{d}\right) \right] \quad (21)$$

and anisotropy plus exchange terms (14,15), can be written as:

$$E_{\text{wall}} = \frac{K}{2} + \frac{\pi^2 A}{d^2}. \quad (22)$$

Minimizing the total energy,  $E_{\text{mag}} + E_{\text{wall}}$ , with respect to  $d$  and equating the result to  $K$  yields the critical thickness  $h'_c$ : for this film thickness the total energies of the stripe domain structure and of a mono-domain state with in-plane magnetization are equal. The corresponding value of the half-period is  $d'_c$ . Both  $h'_c$  and  $d'_c$  depend on the quality ratio,  $Q = 2K/(\mu_0 M_0^2)$ . This dependence can be presented in parametric form by introducing an auxiliary quantity,  $t = \pi h'_c/d'_c$ . One then finds

$$Q = \frac{3}{2} \left[ \frac{1}{t} - \left( \frac{1}{3} + \frac{1}{t} \right) e^{-t} \right], \quad (23)$$

$$\tilde{h}'_c = \sqrt{6} t \sqrt{\frac{1 - (1+t/3)e^{-t}}{1 - (1+t)e^{-t}}}, \quad (24)$$

and

$$\tilde{d}'_c = \pi t^{-1} \tilde{h}'_c. \quad (25)$$

The parameter  $t$  runs from zero to infinity. The resulting  $\tilde{h}'_c$ -vs- $Q$  dependence is displayed in Fig. 4 (dashed curve). It can be regarded as a borderline between the strong- and the weak-stripe phases. The solid line in Fig. 4 presents the exact result of Muller's theory [6, 7],  $\tilde{h}_c(Q)$ . This line separates the region of weak stripes from the area of homogeneous in-plane magnetization, as observed in very thin films with  $Q < 1$ .

For  $Q$  small,  $Q \rightarrow 0$ ,  $t \rightarrow \infty$ , the critical thickness  $\tilde{h}'_c$  diverges,

$$\tilde{h}'_c \approx 3\sqrt{\frac{3}{2}}Q^{-1} \approx 3.67Q^{-1}, \quad (26)$$

whereas

$$\tilde{d}'_c \rightarrow \pi\sqrt{6}. \quad (27)$$

The opposite limiting case is  $t \rightarrow 0$ ,  $Q \rightarrow 1$ . In that limit  $\tilde{h}'_c$  tends to zero,

$$\tilde{h}'_c = 4\sqrt{2(1-Q)}, \quad (28)$$

while  $\tilde{d}'_c$  diverges,

$$\tilde{d}'_c = \pi\sqrt{\frac{2}{1-Q}}. \quad (29)$$

For strong anisotropy,  $Q > 1$  or  $K > \frac{1}{2}\mu_0 M_0^2$ , there is no physically meaningful  $h'_c$  or  $d'_c$  and, without a magnetic field, the mono-domain structure with in-plane magnetization is unstable for any  $h$ . We find it remarkable that our model reproduces the exact value for the critical quality ratio,  $Q = 1$  [6, 7]. The Kittel model is limited to systems with small quality ratios. However, in many strongly anisotropic materials  $Q$  is large and no critical thickness is observed [4, 18, 23].

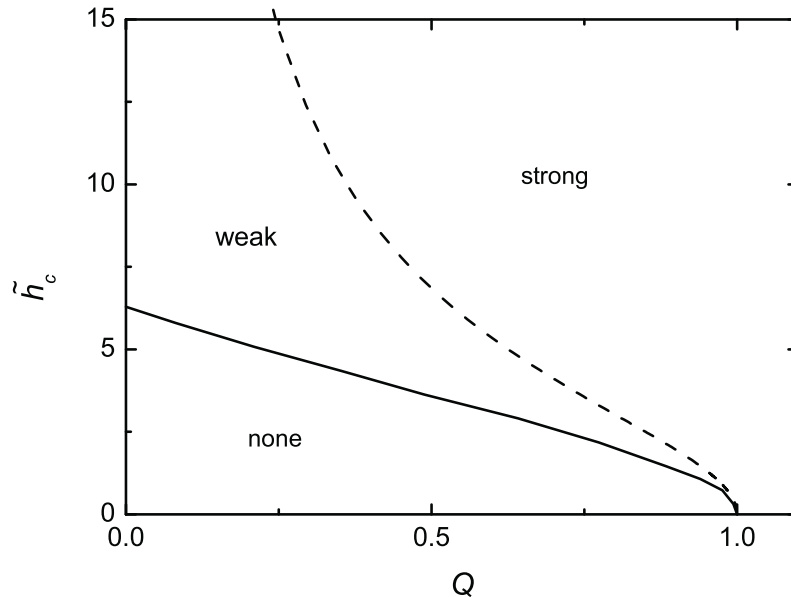


Figure 4: Phase diagram of thin magnetic films in zero magnetic field. The solid line is the critical thickness  $\tilde{h}_c$  obtained in the exact approach [6, 7], it separates the homogeneous state without domains from the weak stripe phase. The dashed line is the reduced critical thickness  $\tilde{h}'_c$  of SWM, computed using Eqs. (23) and (24). This is a cross-over line between the weak and the strong stripe phases.

#### 4.3. Numerical results

Away from the critical region, the total energy (16) has to be minimized with respect to  $d$  and  $\delta$ . In general, for arbitrary  $M_0$ ,  $K$ ,  $A$ , and  $h$ , the result cannot be expressed analytically and we have to resort to a numerical procedure. The dependence on  $A$  and  $K$  can still be taken into account by changing over to the dimensionless variables (2). Then we are left with two quantities  $\tilde{\delta}$  and  $\tilde{d} - \tilde{\delta}$  versus  $\tilde{h}$  with only one parameter  $Q$ . In Fig. 5 we prefer to plot the difference  $\tilde{d} - \tilde{\delta}$  rather than  $\tilde{d}$  since  $\tilde{d} - \tilde{\delta}$  can be regarded as an order parameter. The numerical curves confirm all analytical expressions, in particular, those describing the asymptotic behavior at  $\tilde{h} \gg 1$ , Eqs. (19) and (20). Thus,  $\tilde{\delta}(\tilde{h})$  can be seen to tend to a universal limit.

One observes in Fig. 5 two distinct regimes, for  $Q < 1$  and for  $Q > 1$ . If  $Q > 1$ , the stripe domain structure is stable at any  $\tilde{h}$ . The half-period of the structure,  $d(h)$  or  $\tilde{d}(\tilde{h})$ , has a minimum at a certain finite thickness, increasing towards smaller and larger  $\tilde{h}$ . A prominent feature of the curves with  $Q < 1$  is the presence of a critical thickness  $\tilde{h}'_c$  where the width of the inner domains,  $\tilde{d} - \tilde{\delta}$ , vanishes. At that point the sample contains nothing but domain walls, the magnetic structure being a spiral of period  $2d_c = 2\delta_c$ . Obviously, the wall width cannot be neglected, especially at  $Q \approx 1$ .

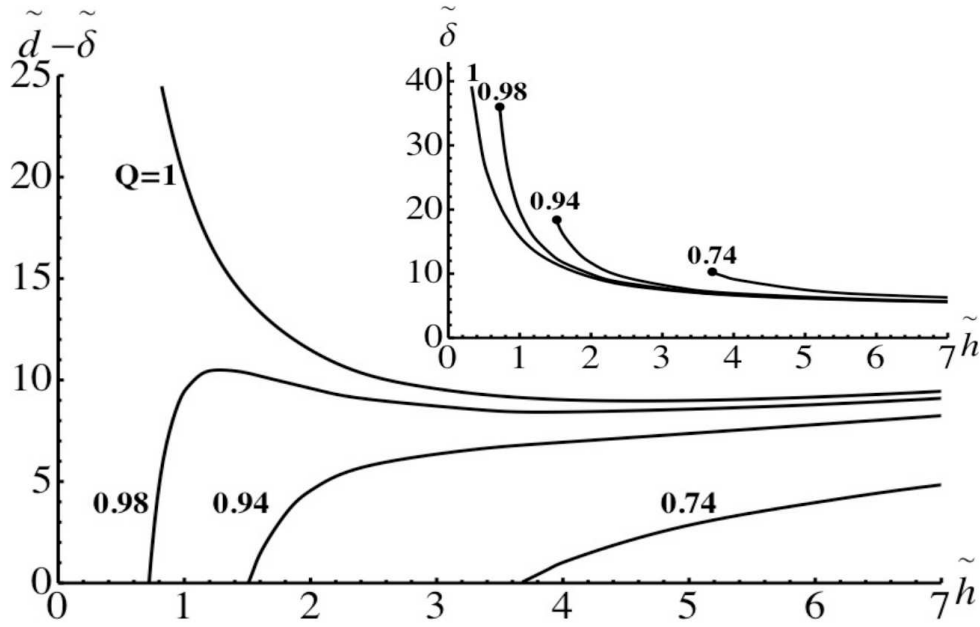


Figure 5: Inner domain width  $\tilde{d} - \tilde{\delta}$  and wall width  $\tilde{\delta}$  as a function of film thickness  $\tilde{h}$ . All figures are presented in reduced coordinates (2). Bold numbers correspond to the value of  $Q$ .

#### 4.4. In-plane remanent magnetization

In a magnetic field directed in the plane of the film the stripe domains arrange themselves parallel to the external field (see Refs. [15, 16]). Each domain wall has a magnetic moment component parallel to the in-plane field direction, all of them being directed in the same sense for a small but finite external field. These contributions sum up to a finite in-plane remanent magnetization with a corresponding hysteresis, as observed in thin *hcp* Co or  $\text{Mn}_5\text{Ge}_3$  films [20, 16]. This remanent in-plane magnetization (when the external field tends to zero) is easy to calculate in our model. The sinewave magnetization profile in the domain wall leads to the following expression:

$$\frac{M_r}{M_0} = \frac{1}{d} \int_0^\delta \sin \frac{\pi x}{\delta} dx = \frac{2\delta}{\pi d}. \quad (30)$$

At the critical thickness, the remanent magnetization is equal to  $2/\pi \simeq 63.7\%$  of the saturation magnetization. Just below this point we would expect the weak stripe phase [14] in a narrow interval of thicknesses before the transition into the planar mono-domain state. In the weak stripe phase the maximum  $z$ -component of the magnetization is less than  $M_0$ , like in sawtooth magnetization model [14]. However, the weak stripe phase is beyond the scope of our model.

## 5. Hexagonal Co

Cobalt hexagonal thin films have been intensively studied. Below a critical thickness, such films exhibit planar magnetization. Recent experimental publications [17, 16, 24] report critical thicknesses between 25 and 50 nanometers. Since the study of Brandenburg *et al.* [17] is the most complete one, SWM has been tested using those data, especially the half-period as a function of film thickness, shown in Fig. 6.

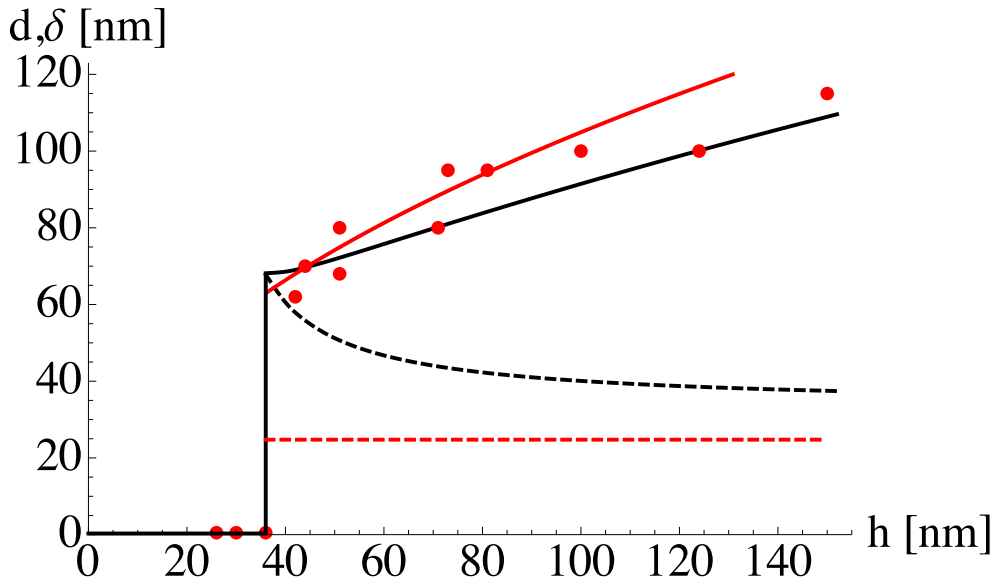


Figure 6: Half-period  $d$  (full line) and wall width  $\delta$  (dashed line) as functions of thickness for Co films. Red points are experimental  $d$  values from Ref. [17]. Red and black curves are fits to the Kittel model and SWM, respectively.

SWM has three parameters to characterize different materials: the magneto-crystalline anisotropy constant  $K$ , the saturation magnetization  $M_0$  and the exchange stiffness constant  $A$ . The saturation magnetization was fixed to the experimental value of  $M_0 = 1.43$  MA/m, while the anisotropy as well as the exchange constant were chosen as fitting parameters. The best fit was obtained with  $K = 820$  kJ/m<sup>3</sup>, which is rather close to the bulk anisotropy constant (see Tab. 1), and  $A = 45$  pJ/m, which exceeds the value deduced from inelastic neutron scattering experiments [26]. However, it should be taken into account that  $A$  is not known accurately, since relating neutron scattering data with our continuum model involves several approximations.

For comparison, we also fitted the experimental data to the Kittel model (see Fig. 6), leading to the parameter values presented in Table 1. The saturation magnetization was fixed to the same value, but the anisotropy and exchange constants deviate more strongly from the experiment than those obtained in the SWM fit. This suggests that the Kittel model is less realistic than SWM. We also observe important differences between both models near the critical thickness. The curvature of  $d(h)$  near  $h_c$  is different in the two models. In SWM, for  $h$  between 40 and 80 nm the wall is wider than the inner domain, whereas in the Kittel model the wall width remains

cobalt	Kittel	SWM	measurements
$K$ [kJ/m <sup>3</sup> ]	1200	820	820 <sup>a</sup> , 920 <sup>b</sup>
$A$ [pJ/m]	76	45	28 <sup>c</sup>
$M_0$ [MA/m]	1.43*	1.43*	1.43 <sup>d</sup>
$h_c$ [nm]	36	36	36 ± 3
$d_c$ [nm]	63	67	63 ± 5

Table 1: Summary of important physical constants obtained for cobalt. The asterisks indicate fixed parameters. Experimental data are extracted from: <sup>a</sup> Ref. [27], <sup>b</sup> Ref. [15], <sup>c</sup> Ref. [26], <sup>d</sup> Ref. [17, 25]

constant and always inferior to the inner domain width.

The quality factor for Co is  $Q = 0.64$ , which is less than one. We expect that for materials with stronger anisotropy, i.e. with larger  $Q$ , the difference between SWM and the Kittel model will be even more significant.

## 6. Comparison

Our model is constructed in such a way that it applies at any  $Q$ , including the strong-anisotropy case,  $Q > 1$ , where there is no critical thickness.

The most interesting region is the one of medium anisotropy,  $\frac{1}{2} \lesssim Q < 1$ . To illustrate that region, we chose hexagonal cobalt as an example. With the parameters of Table 1 (SWM) we evaluated the critical thickness in SWM,  $h'_c = 36$  nm. This agrees with the experiment of Brandenburg et al. [17], who find a critical thickness of about 40 nm. However, in Muller's exact theory [6] the critical thickness comes out much smaller,  $h_c = 23$  nm. One has to take into account, though, that stripe domains were observed by other groups in Co films as thin as 25 nm and that weak stripes are certainly hard to see. Our interpretation is that the interval between Muller's  $h_c = 23$  nm and the SWM  $h'_c = 36$  nm is a region of the weak stripe phase.

In the case of cobalt, such an interpretation is supported by a calculation of the weak stripe phase within the sawtooth magnetization model. The two variational parameters are the maximum canting angle  $\Theta_0$  and the half-period  $d$ . For better precision, we included the complete Fourier series as well as the magnetostatic interaction between the top and bottom surfaces. The numerical results are presented in Fig. 7. The weak stripe phase sets in at  $h = 28$  nm and has a lower energy than the strong stripe phase up to 44 nm. Between 28 nm and 44 nm the maximum canting angle increases from zero to 76 degrees. So, in the case of hexagonal cobalt, we would expect the existence of the weak stripe phase between 23 and about 44 nm. At larger thicknesses the strong stripe phase prevails and SWM is more appropriate than the sawtooth magnetization model.

Let us now briefly discuss the region of very small anisotropy,  $Q \ll 1$ . It allows mathematical simplifications, as already discussed in Section 4. There, it was shown that the range of thicknesses where the weak stripe phase could be expected becomes wider according as  $Q$  decreases, i.e. as the magnetic anisotropy weakens. For very weak anisotropy we also expect other complications, such as the presence of closure domains. We believe our model can still be applied if the layer of the closure domains

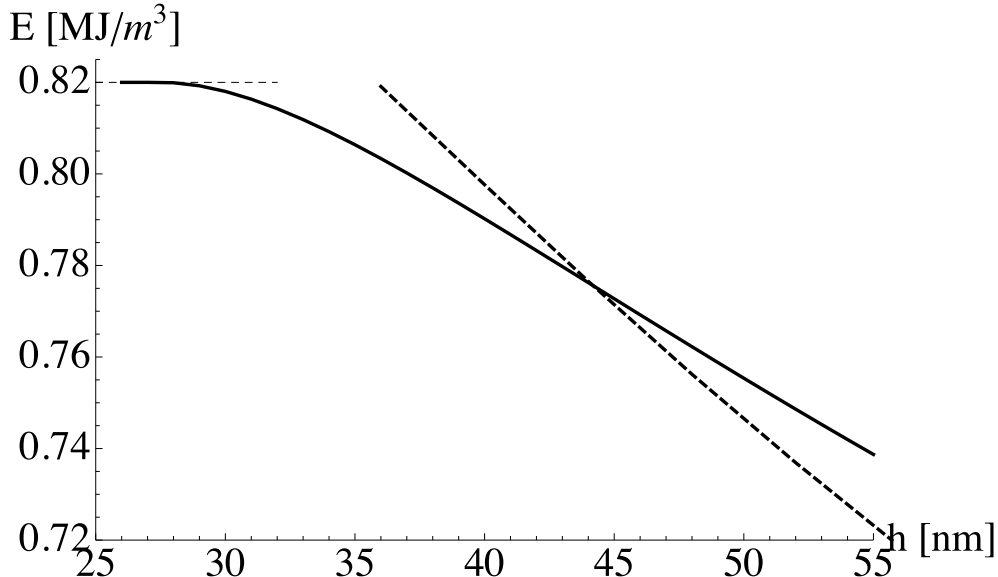


Figure 7: Comparison of the total energy of the weak stripe phase (sawtooth magnetization model, solid line) with that one of the strong stripe phase (SWM, dashed line).

is much thinner than the film as a whole.

## 7. Conclusion

We present a model (SWM) for the strong stripe phase in magnetic thin films with perpendicular anisotropy, which improves the well-known Kittel model in two respects. Firstly, our model includes the magnetostatic interaction between the top and bottom surfaces of the film. This is important for materials with strong magnetocrystalline anisotropy. Secondly, the domain walls are treated explicitly, which improves the numerical accuracy and allows the calculation of the in-plane remanent magnetization. Our model is simple, but general enough to permit a thorough analysis of the strong stripe phase. It is especially suited to interpret experimental data. We demonstrate the existence of a critical anisotropy above which stripe domains exist at any film thickness. SWM reproduces the exact threshold value,  $Q = 1$ . We derive a number of analytical results facilitating the estimation of important parameters. The numerical results obtained for different quality factors  $Q$  show the evolution of domain and wall widths as functions of film thickness.

With the new model we are able to correctly describe the behavior of magnetic domains in cobalt thin films. It allows to explain the experimental observations of Brandenburg *et al* [17] with more realistic fitting parameters than using the Kittel model. By comparing the exact critical thickness for stripe nucleation  $h_c$  with our critical thickness  $h'_c$ , which corresponds to the on-set of strong stripes, we are able to estimate the range of thicknesses where weak stripes are expected. We show that for Co this interval is rather narrow, 10 to 15 nm, which validates our model. We should

remark that the currently available experimental data for Co do not suffice for locating the thickness range of the weak stripe phase accurately. We find it important that our model takes the wall width into account in an adequate way. In the neighborhood of the critical thickness, domain and wall width are of comparable size. Thanks to its universality, our model can be applied to other types of ferromagnetic films, e.g., FePd or Mn<sub>5</sub>Ge<sub>3</sub>.

### Acknowledgments

This work was supported by PICS project (No. 4767) and by ANR-project MNGE-SPIN. The authors are grateful to A.N. Bogdanov for illuminating discussions.

### References

- [1] Kittel C 1946 *Phys. Rev.* **70** 965
- [2] Málek Z and Kamberský V 1958 *Czech. J. Phys.* **8** 416
- [3] Kooy C and Enz U 1960 *Philips Res. Rep.* **15** 7
- [4] Gehanno V, Samson Y, Marty A, Gilles B and Chamberod A 1997 *J. Magn. Magn. Mater.* **172** 26
- [5] Kiselev N S, Bran C, Wolff U, Schultz L, Bogdanov A N, Hellwig O, Neu V, and Rößler 2010 *Phys. Rev. B* **81** 054409
- [6] Muller M W 1961 *Phys. Rev.* **122** 1485
- [7] Hubert A and Schäfer R 1998 *Magnetic domains: the analysis of magnetic microstructures* (Springer, Berlin)
- [8] Labrune M and Thiaville A 2001 *Eur. Phys. J. B* **23** 17
- [9] Kisielewski M, Maziewski A, Polyakova T and Zablotksii V 2004 *Phys. Rev. B* **69** 184419
- [10] Kisielewski M, Maziewski A and Zablotksii V 2007 *J. Magn. Magn. Mater.* **316** 277
- [11] Zhao G P, Chen L and Wang J 2009 *J. Appl. Phys.* **105** 061601
- [12] Sukstanskii A L and Primak K I 1997 *J. Magn. Magn. Mater.* **169** 31
- [13] Marty A, Samson Y, Gilles B, Belakhovsky M, Dudzik E, Dürr H, Dhési S S, van der Laan G and Goedkoop J B 2000 *J. Appl. Phys.* **87** 5472
- [14] Saito N, Fujiwara H and Sugita Y 1964 *J. Phys. Soc. Jpn* **19** 1116
- [15] Hehn M, thesis, <http://tel.archives-ouvertes.fr/tel-00002760/>
- [16] Hehn M, Padovani S, Ounadjela K and Bucher J P 1996 *Phys. Rev. B* **54** 3428
- [17] Brandenburg J, Hühne R, Schultz L and Neu V 2009 *Phys. Rev. B* **79** 054429
- [18] Gemperle R, Murtinová L and Kamberský V 1996 *Phys. Status Solidi (a)* **158** 229
- [19] Olive-Mendez S F *et al* 2008 *Thin Solid Films* **517** 191
- [20] Spiesser A *et al* 2010 *Thin Solid Films* **518** S113
- [21] E. Trémolet de Lacheisserie 1999 *Magnétisme, tome I* (collection Grenoble Sciences)
- [22] Landau L and Lifchitz E 1969 *Électrodynamique des milieux continus, tome VIII, chap. 5, §44* (éditions MIR, Moscou)
- [23] Yang Y, Chen J S, and Chow G M 2011 *J. Appl. Phys.* **109** 07B744
- [24] Donzelli O, Bassani M, Spizzo F and Palmeri D 2008 *J. Magn. Magn. Mater.* **320** e261
- [25] Donnet D M, Krishnan K M and Yajima Y 1995 *J. Phys. D: Appl. Phys.* **28** 1942
- [26] Vaz C A F, Bland J A C and Lauhoff G 2008 *Rep. Prog. Phys.* **71** 056501
- [27] Paige D, Szpunar B and Tanner B K 1984 *J. Magn. Magn. Mater.* **44** 239